Int J Thermophys (2008) 29:2088–2101
DOI 10.1007/s10765-008-0531-9

Design of Experiment for Thermal Diffusivity Measurements of Composite Material with Orthogonal Anisotropy

J. Beňačka · L. Vozár · I. Štubňa

Published online: 15 November 2008
© Springer Science+Business Media, LLC 2008

Abstract This article deals with simultaneous measurements of three mutually orthogonal thermal diffusivities of a material with orthogonal anisotropy using the flash method. Unlike the conventional flash method, the modified measuring technique considers pulse heating over a rectangular area of the front face of a wall-shaped sample of an orthotropic composite material. The thermal diffusivities are calculated analyzing the temperature rise versus time evolutions when measured simultaneously at various positions on the sample surface. This article presents a data reduction method that enables estimates of the thermal diffusivities for the three principal axes. The theory takes into account heat losses from the front and rear faces. The results of an experimental design analysis are discussed.

Keywords Data reduction · Laser-flash method · Orthogonal anisotropy · Sensitivity · Thermal diffusivity

1 Introduction

The flash method [1] has become the most popular experimental method for measuring the thermal diffusivity. In this method, the front face of a small wall-shaped sample receives a pulse of radiant energy coming from either a laser or a flash lamp. The thermal diffusivity value is computed from the resulting temperature response on the opposite (rear) face of the sample. Although the method was originally developed for measurement of homogeneous isotropic opaque materials, it has been successfully applied to advanced materials—composites, layered structures, semitransparent

J. Beňačka · L. Vozár (✉) · I. Štubňa
Department of Physics, Faculty of Natural Sciences,
Constantine the Philosopher University, Tr. A. Hlinku 1,
94974 Nitra, Slovakia
e-mail: LVozar@ukf.sk

media, and materials with a significant dependence of the thermophysical properties on temperature [2–4].

The radial heat flow modification of the flash method enables simultaneous measurements of the axial thermal diffusivity (across the sample) and the radial thermal diffusivity (parallel to the front and rear surfaces) of an anisotropic material with cylindrical symmetry. The technique uses a heat pulse induced by irradiating the sample front face in a central circular area of radius smaller than the sample radius. The

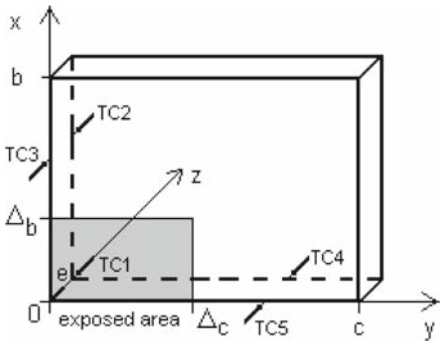

Fig. 1 Upper-right-hand quadrant of the parallelepiped considered in the analytical model and the positions of thermocouples in experiment

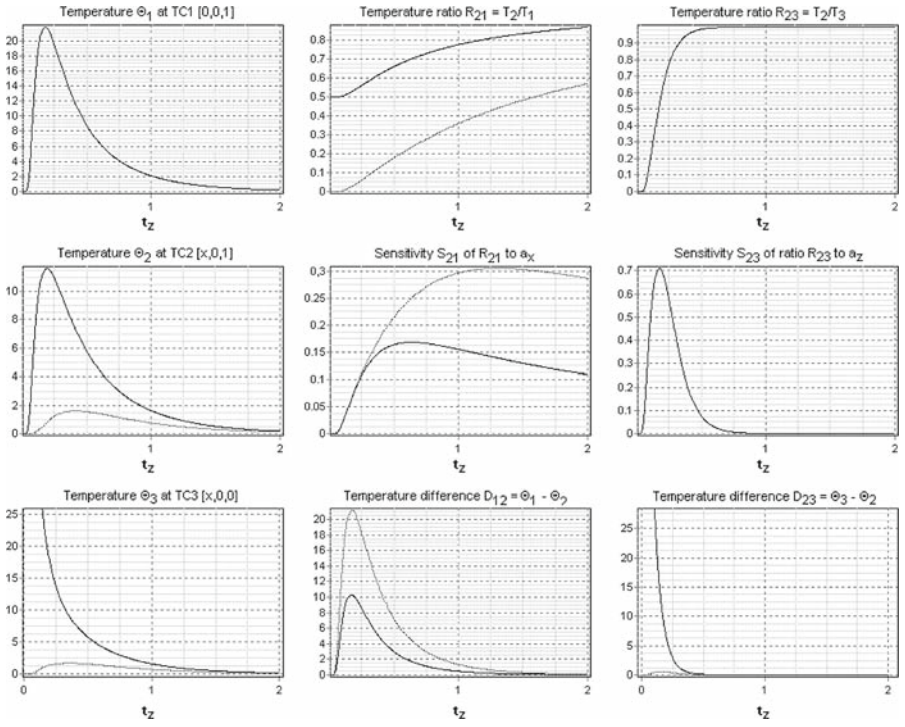

Fig. 2 Functions Θ_1, Θ_2, Θ_3, R_{21}, S_{21}, D_{12}, R_{23}, S_{23}, D_{23} at $e/b = 0.2$, $H = 1$, $a_x/a_z = 0.2$, $a_y/a_z = 1$, $\bar{\Delta}_b = 0.1$; normal line: $\bar{x} = 0.1$, small-dotted line: $\bar{x} = 0.2$

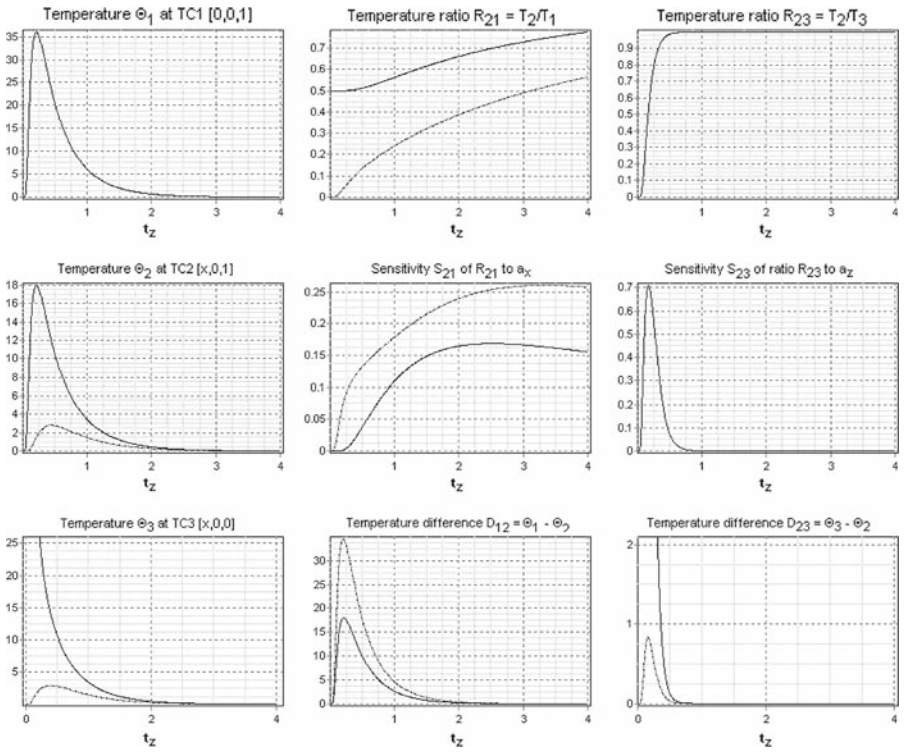

Fig. 3 Functions Θ_1, Θ_2, Θ_3, R_{21}, S_{21}, D_{12}, R_{23}, S_{23}, D_{23} at $e/b = 0.2$, $H = 1$, $a_x/a_z = 0.2$, $a_y/a_z = 1$, $\bar{\Delta}_b = 0.2$; normal line: $\bar{x} = 0.2$, small-dotted line: $\bar{x} = 0.3$

temperature response is monitored on the rear face at two different distances from the center. Both axial and radial thermal diffusivities are simultaneously deduced from the recorded experimental temperature versus time data [5,6].

To overcome the significant influence of the temperature sensor position on the estimation of the radial diffusivity [7], an application of further detectors has been proposed [8]. Another method uses adjustment of the position of the detector in the data reduction procedure [9]. An optimal design of the experiment has been performed as well [10].

A generalization of the flash technique for measurement of three mutually orthogonal thermal diffusivities in orthotropic finite and semi-infinite solids has been elaborated [11]. In this method, a central square area of the sample front face is irradiated, and the temperature response is monitored on the rear face at different locations. As demonstrated, the ratio of these temperature evolutions gives sufficient information to measure an in-plane thermal diffusivity. The primary interest for preferring this kind of an orthotropic model to that based on the cylindrical symmetry assumption derives from the fact that the model is much more suitable for investigating oriented composite structures, i.e., materials reinforced with fibers. An analytical model that takes into account heat transfer between the sample and its environment has been derived [12].

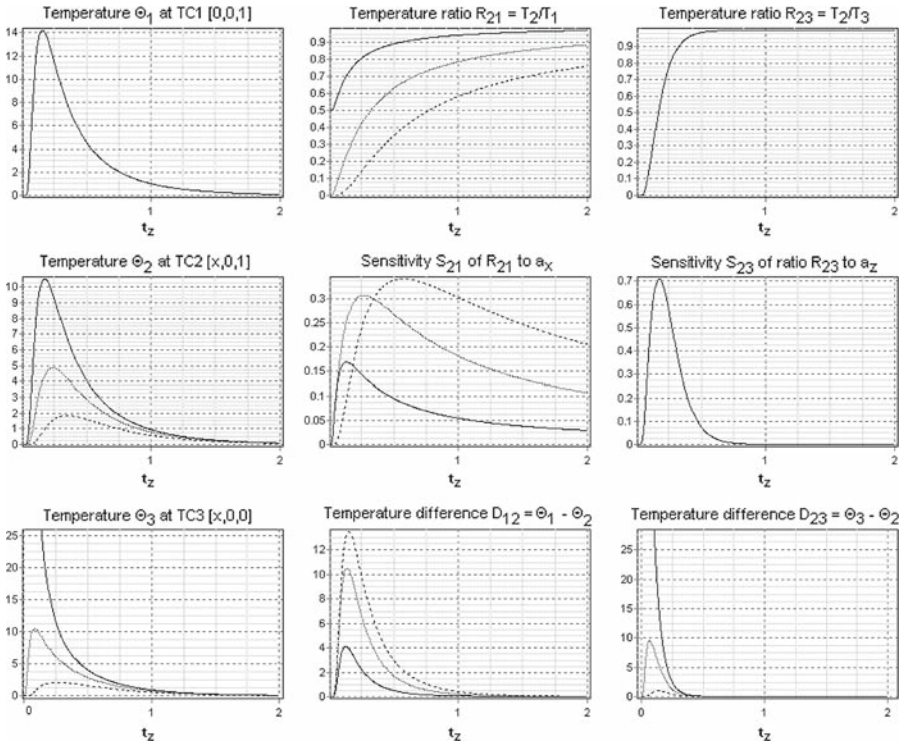

Fig. 4 Functions $\Theta_1, \Theta_2, \Theta_3, R_{21}, S_{21}, D_{12}, R_{23}, S_{23}, D_{23}$ at $e/b = 0.2, H = 1, a_x/a_z = 1, a_y/a_z = 1$, $\bar{\Delta}_b = 0.1$; normal line: $\bar{x} = 0.1$, small-dotted line: $\bar{x} = 0.2$, dotted line: $\bar{x} = 0.3$

This article deals with simultaneous estimation of thermal diffusivities in an orthotropic material for all the three principal axes. This method uses the theory that takes into account of heat losses from the front and rear faces of the sample. An optimal experimental design is analyzed and discussed.

2 Theory

Let us consider an orthotropic parallelepiped of length $2b$, width $2c$, and thickness e initially at constant zero temperature. Let the geometric axes conform to the principal axes of the orthotropic material of thermal diffusivities a_x, a_y, and a_z. Let the heated area be a rectangle of size $2\Delta_b \times 2\Delta_c$, located symmetrically around the center of the front face ($z = 0$), its sides in parallel with x and y axes. Let it be subjected to an instantaneous heat pulse of energy Q at time $t = 0$. Because of the symmetry along the x and y axes, we consider only the upper-right quadrant of the sample, i.e., the parallelepiped of $b \times c$ and thickness e (Fig. 1). It is assumed that the surfaces at $x = 0$, $x = b$, $y = 0$, and $y = c$ are thermally insulated, and that there are equal heat losses at $z = 0$ and $z = e$ governed by the Biot number $H (H = he/k_z$, where h is

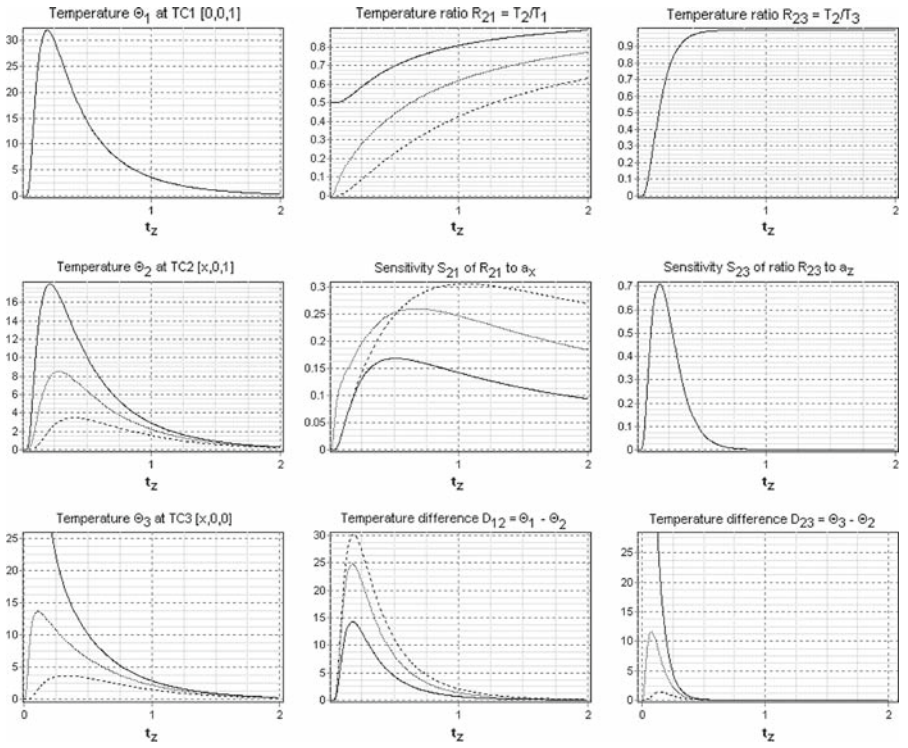

Fig. 5 Functions $\Theta_1, \Theta_2, \Theta_3, R_{21}, S_{21}, D_{12}, R_{23}, S_{23}, D_{23}$ at $e/b = 0.2$, $H = 1$, $a_x/a_z = 1$, $a_y/a_z = 1$, $\bar{\Delta}_b = 0.2$; normal line: $\bar{x} = 0.2$, small-dotted line: $\bar{x} = 0.3$, dotted line: $\bar{x} = 0.4$

the heat transfer coefficient and k_z is the thermal conductivity in the z direction). The dimensionless temperature rise Θ of the parallelepiped conforms to [12]

$$\Theta(\bar{x}, \bar{y}, \bar{z}, t) = \frac{T(\bar{x}, \bar{y}, \bar{z}, t)}{T_{\lim}} = \left[1 + 2\sum_{k=1}^{\infty} \cos(k\pi\bar{x}) \frac{\sin(k\pi\bar{\Delta}_b)}{k\pi\bar{\Delta}_b} \exp\left(-\pi^2 k^2 t_x\right)\right] \times \left[1 + 2\sum_{m=1}^{\infty} \cos(m\pi\bar{y}) \frac{\sin(m\pi\bar{\Delta}_c)}{m\pi\bar{\Delta}_c} \exp\left(-\pi^2 m^2 t_y\right)\right] \times \sum_{n=1}^{\infty} a_n \left[\cos(u_n\bar{z}) + \frac{H}{u_n} \sin(u_n\bar{z})\right] \exp\left(-u_n^2 t_z\right) \quad (1)$$

where T is the temperature rise, $T_{\lim} = Q/\rho cabe$ is the adiabatic limit temperature rise, i.e., the temperature the sample reaches for the case of adiabatic boundary conditions, ρ is the density, c is the heat capacity,

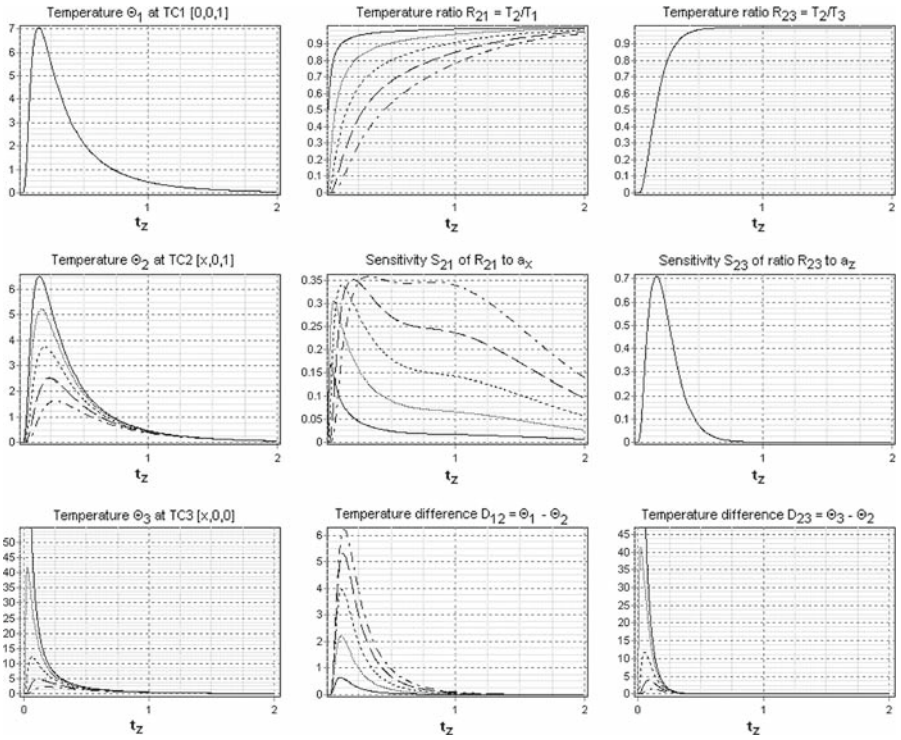

Fig. 6 Functions $\Theta_1, \Theta_2, \Theta_3, R_{21}, S_{21}, D_{12}, R_{23}, S_{23}, D_{23}$ at $e/b = 0.2$, $H = 1$, $a_x/a_z = 5$, $a_y/a_z = 1$, $\bar{\Delta}_b = 0.1$; normal line: $\bar{x} = 0.1$, small-dotted line: $\bar{x} = 0.2$, dotted line: $\bar{x} = 0.3$, dashed line: $\bar{x} = 0.4$, dashed-dotted line: $\bar{x} = 0.5$

$$\bar{x} = \frac{x}{b}, \quad \bar{y} = \frac{y}{c}, \quad \bar{z} = \frac{z}{e}, \quad \bar{\Delta}_b = \frac{\Delta_b}{b}, \quad \bar{\Delta}_c = \frac{\Delta_c}{c}, \tag{2}$$

$$t_x = \frac{a_x t}{b^2} = \frac{a_x}{a_z}\frac{e^2}{b^2} t_z, \tag{3}$$

$$t_y = \frac{a_y t}{c^2} = \frac{a_y}{a_z}\frac{e^2}{c^2} t_z, \tag{4}$$

$$t_z = \frac{a_z t}{e^2}, \tag{5}$$

and

$$a_n = \frac{2u_n^2}{u_n^2 + H^2 + 2H}. \tag{6}$$

u_n is the nth positive root of

$$(u^2 - H^2)\tan(u) = 2Hu. \tag{7}$$

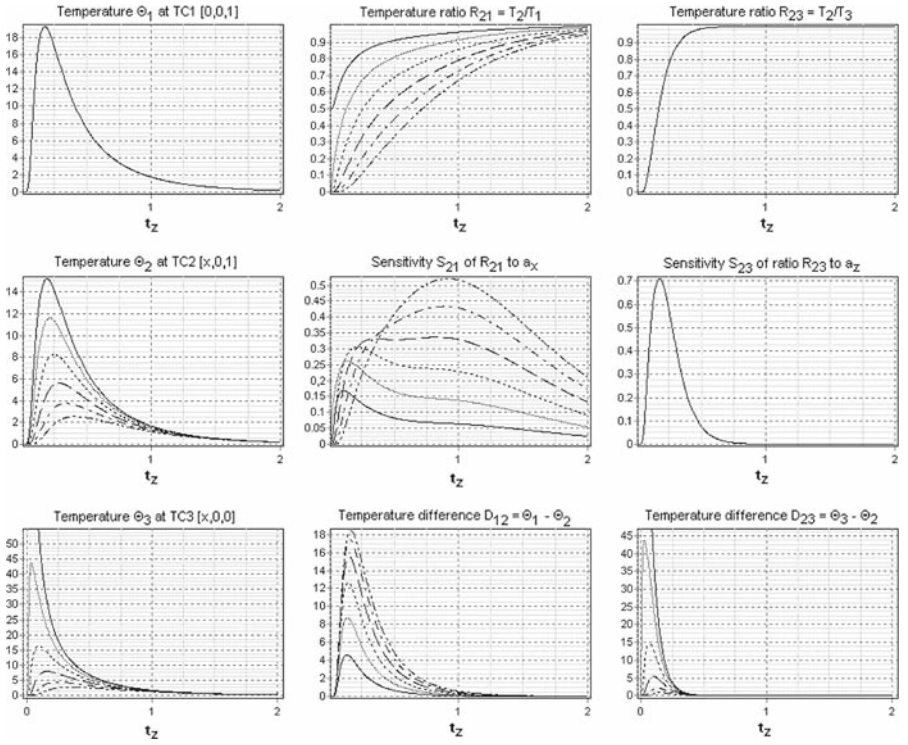

Fig. 7 Functions $\Theta_1, \Theta_2, \Theta_3, R_{21}, S_{21}, D_{12}, R_{23}, S_{23}, D_{23}$ at $e/b = 0.2$, $H = 1$, $a_x/a_z = 5$, $a_y/a_z = 1$, $\bar{\Delta}_b = 0.2$; normal line: $\bar{x} = 0.2$, small-dotted line: $\bar{x} = 0.3$, dotted line: $\bar{x} = 0.4$, dashed line: $\bar{x} = 0.5$, dashed-dotted line: $\bar{x} = 0.6$, dashed-dotted-dotted line: $\bar{x} = 0.7$

We note that the dimensionless temperature rise Θ achieves the steady-state limiting value equal to one in the case of negligible heat losses ($H = 0$) after long time ($t \to \infty$).

Equation 1 is the working equation for data reduction, i.e., calculation of the thermal diffusivities. For practical reasons, it is much easier to set the screening for the heat pulse than to adjust the pulse energy over a wide range.

3 Principles of the Measurement

The estimation of thermal diffusivities a_x, a_y, and a_z requires knowledge of the temperature response after the heat pulse is irradiated on the front face. Because of sample geometry and symmetry of Eq. 1, we describe the estimation of the thermal diffusivity in two directions only–the in-plane thermal diffusivity a_x and the cross thermal diffusivity a_z. The estimation of the in-plane diffusivity a_y can be made in the same way as the estimation of the diffusivity a_x.

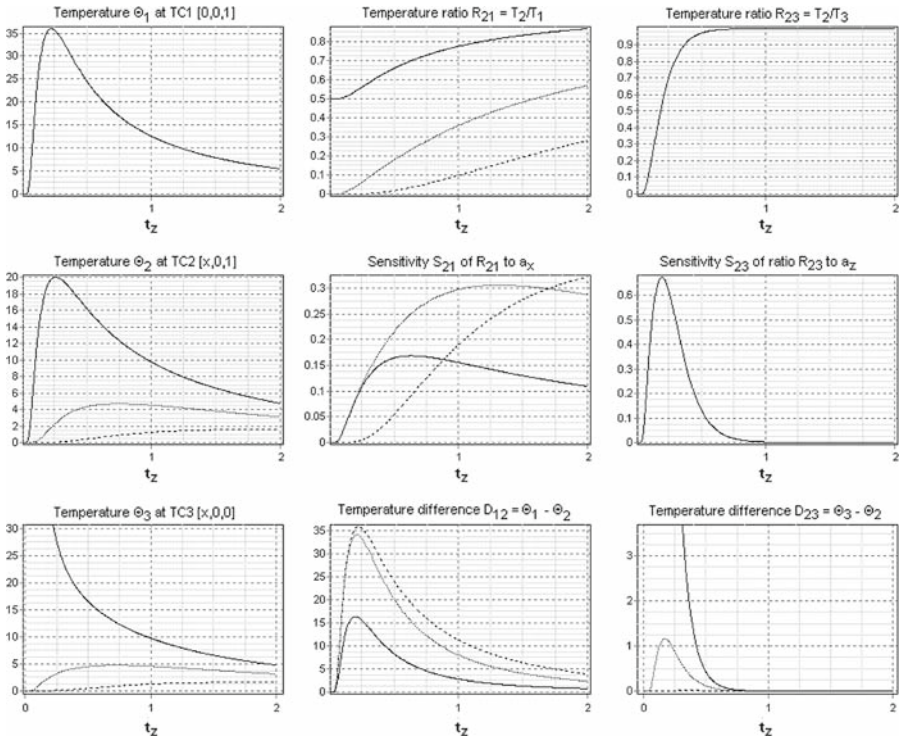

Fig. 8 Functions Θ_1, Θ_2, Θ_3, R_{21}, S_{21}, D_{12}, R_{23}, S_{23}, D_{23} at $e/b = 0.2$, $H = 0.1$, $a_x/a_z = 0.2$, $a_y/a_z = 1$, $\bar{\Delta}_b = 0.1$; normal line: $\bar{x} = 0.1$, small-dotted line: $\bar{x} = 0.2$, dotted line: $\bar{x} = 0.3$

The proposed method considers three temperature sensors (thermocouples) TC1, TC2, and TC3 located at positions $[0, 0, 1]$, $[\bar{x}, 0, 1]$, and $[\bar{x}, 0, 0]$ $(0 < \bar{x} < 1)$, respectively as shown in Fig. 1. Position TC1 corresponds to the center of the sample rear face. TC2 and TC3 are located on the x-axis on the rear and front faces, respectively. Let temperatures T_1, T_2, and T_3 correspond to those measured by sensors TC1, TC2, and TC3. Using Eqs. 1–7, ratios $R_{21} = T_2/T_1$ and $R_{23} = T_2/T_3$ can be expressed as follows:

$$R_{21}\left(\bar{\Delta}_b, \bar{x}, t_z\right) = \frac{T_2}{T_1} = \frac{\Theta_2}{\Theta_1} = \frac{1 + 2\sum_{k=1}^{\infty} \cos\left(k\pi\bar{x}\right) \frac{\sin\left(k\pi\bar{\Delta}_b\right)}{k\pi\bar{\Delta}_b} \exp\left(-\pi^2 k^2 \frac{a_x}{a_z}\frac{e^2}{b^2} t_z\right)}{1 + 2\sum_{k=1}^{\infty} \frac{\sin\left(k\pi\bar{\Delta}_b\right)}{k\pi\bar{\Delta}_b} \exp\left(-\pi^2 k^2 \frac{a_x}{a_z}\frac{e^2}{b^2} t_z\right)}, \tag{8}$$

$$R_{23}\left(H, t_z\right) = \frac{T_2}{T_3} = \frac{\Theta_2}{\Theta_3} = \frac{\sum_{n=1}^{\infty} a_n \left[\cos\left(u_n\right) + \frac{H}{u_n}\sin\left(u_n\right)\right] \exp\left(-u_n^2 t_z\right)}{\sum_{n=1}^{\infty} a_n \exp\left(-u_n^2 t_z\right)}. \tag{9}$$

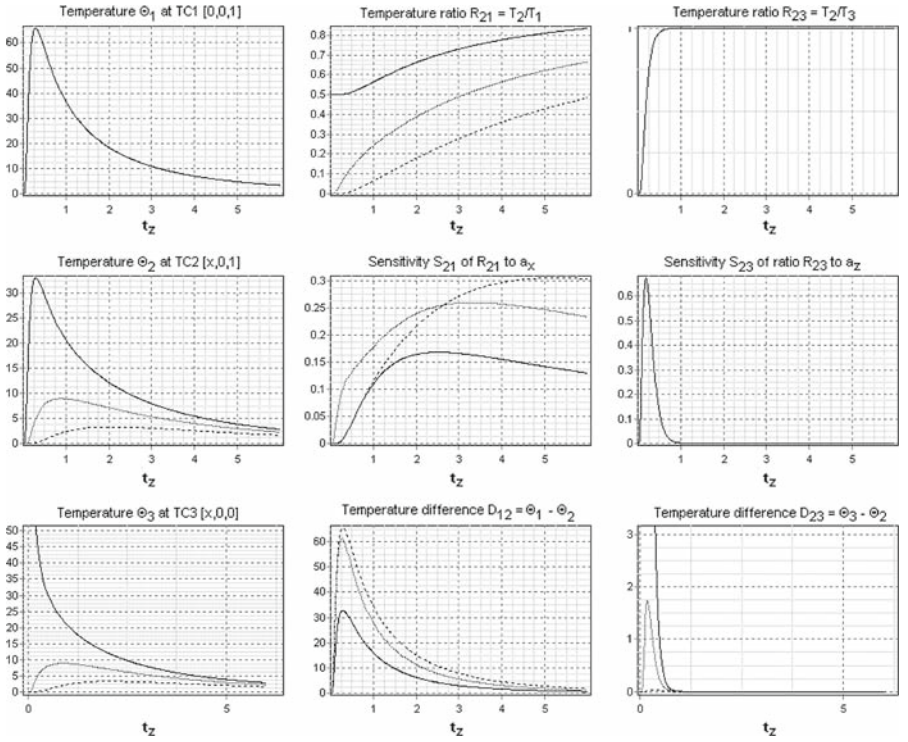

Fig. 9 Functions Θ_1, Θ_2, Θ_3, R_{21}, S_{21}, D_{12}, R_{23}, S_{23}, D_{23} at $e/b = 0.2$, $H = 0.1$, $a_x/a_z = 0.2$, $a_y/a_z = 1$, $\bar{\Delta}_b = 0.2$; normal line: $\bar{x} = 0.2$, small-dotted line: $\bar{x} = 0.3$, dotted line: $\bar{x} = 0.4$

The sensitivity of R_{21} to a_x is

$$S_{21}\left(\bar{\Delta}_b, \bar{x}, t_z\right) = \frac{\partial R_{21}}{\partial a_x} a_x = \frac{\partial R_{21}}{\partial t_x} \frac{\partial t_x}{\partial a_x} a_x = \frac{\partial R_{21}}{\partial t_x} t_x = \frac{\partial R_{21}}{\partial t_z} \frac{\partial t_z}{\partial t_x} t_x = \frac{\partial R_{21}}{\partial t_z} t_z, \quad (10)$$

and the sensitivity of R_{23} to a_z is

$$S_{23}\left(H, t_z\right) = \frac{\partial R_{23}}{\partial a_z} a_z = \frac{\partial R_{23}}{\partial t_z} \frac{\partial t_z}{\partial a_z} a_z = \frac{\partial R_{23}}{\partial t_z} \frac{t}{b^2} a_z = \frac{\partial R_{23}}{\partial t_z} t_z. \quad (11)$$

We consider a sample with square faces ($b = c$) of maximum ratio $e/b = 0.2$. (The area of the sides is $1/6 = 16.67\,\%$ of the entire surface.).

We assume H ranges from 0 to 1, and sensitivity ratios a_x/a_z, a_y/a_z, and a_x/a_y range from 1/5 to 5/1 each. The worst case is when $a_x/a_z = 1/5 = 0.2$, $a_y/a_z = 1$ (most of the heat diffuses in y direction), and $H = 1$ (big heat losses from the faces). There is a question then whether temperatures rises T_1, T_2, and T_3 are large enough to be measured in the experiment.

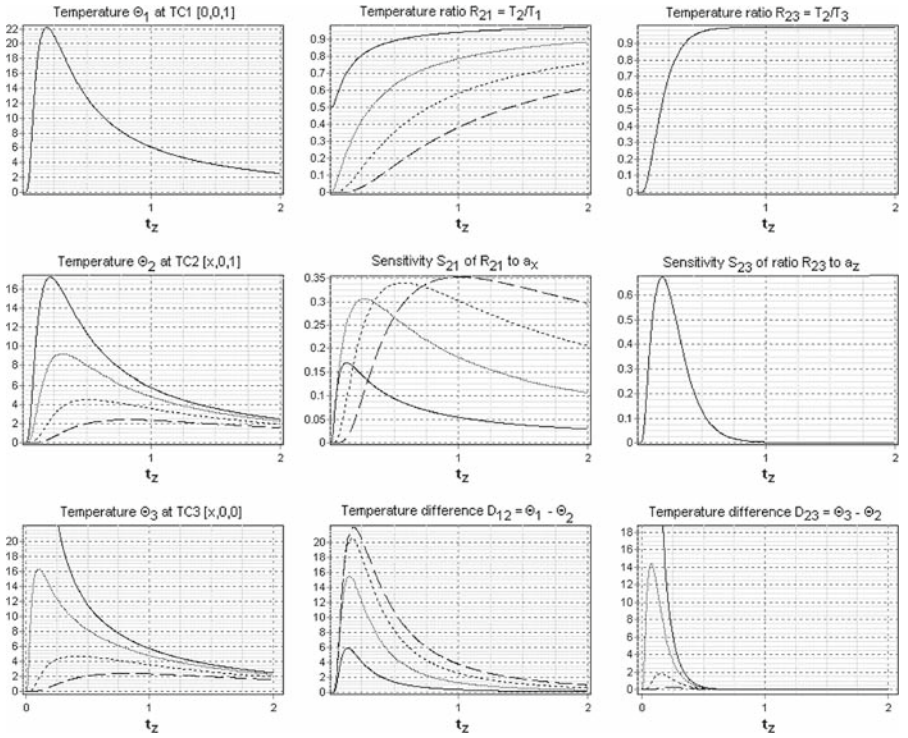

Fig. 10 Functions Θ_1, Θ_2, Θ_3, R_{21}, S_{21}, D_{12}, R_{23}, S_{23}, D_{23} at $e/b = 0.2$, $H = 0.1$, $a_x/a_z = 1$, $a_y/a_z = 1$, $\bar{\Delta}_b = 0.1$; normal line: $\bar{x} = 0.1$, small-dotted line: $\bar{x} = 0.2$, dotted line: $\bar{x} = 0.3$, dashed line: $\bar{x} = 0.4$

We assume that the delivered energy Q is sufficient to cause T_{lim} to be measurable, which means that $\Theta = 1$ is measurable. The most interesting time points are $t_{z\,S21\,\max}$ and $t_{z\,S23\,\max}$, when sensitivities S_{21} and S_{23} reach a maximum. Then, functions Θ_1, Θ_2, and Θ_3 have to produce values around 1 to be measurable. Moreover, we introduce checking functions $D_{12} = \Theta_1 - \Theta_2$ and $D_{32} = \Theta_3 - \Theta_2$ that have to satisfy this rule, as well.

Functions R_{21}, R_{23}, S_{21}, and S_{23} (Eqs. 8–11) do not depend on the delivered energy Q, but temperatures T_1, T_2, and T_3 do. If we consider a constant planar energy flow from the source, then enlarging $\bar{\Delta}_b$ twice causes an increase in Q, and consequently the temperatures by a factor of four. We apply this rule for computing Θ_1, Θ_2, Θ_3, D_{12}, and D_{32} to simulate the real heating, starting at reference point $\bar{\Delta}_b = 0.1$.

Let $e/b = 0.2$, $a_x/a_z = 0.2, 1, 5$, respectively, $a_y/a_z = 1$, $H = 1, 0.1$, respectively, $\bar{\Delta}_b$ varies from 0.1 to 0.9, and $\bar{x}$ varies from $\bar{\Delta}_b + 0.1$ to 1 for each $\bar{\Delta}_b$. We are looking for maximum S_{21}, S_{23} at measurable Θ_1, Θ_2, Θ_3, D_{12}, and D_{32}. The analysis is shown in Figs. 2, 3, 4, 5, 6, 7, 8, 9, 10, 11, 12, 13, 14. In most cases, a smaller heating area causes more sensible measurements of the radial diffusivities (with respect to the measurability of the temperatures). In most cases, we can take $\bar{\Delta}_b = 0.1$ and $\bar{x} = 0.2$ for the optimal values. Then $S_{21\,\max} \approx 0.3$ and $S_{23\ \max} \approx 0.7$. For larger $\bar{\Delta}_b$ and $\bar{x}$,S_{21}

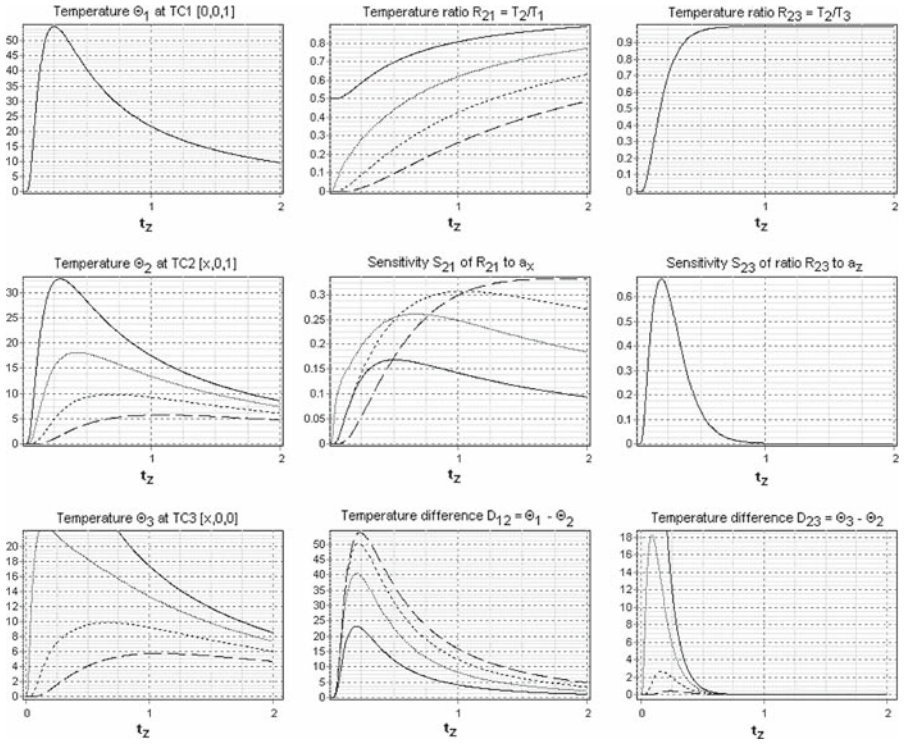

Fig. 11 Functions Θ_1, Θ_2, Θ_3, R_{21}, S_{21}, D_{12}, R_{23}, S_{23}, D_{23} at $e/b = 0.2$, $H = 0.1$, $a_x/a_z = 1$, $a_y/a_z = 1$, $\bar{\Delta}_b = 0.2$; normal line: $\bar{x} = 0.2$, small-dotted line: $\bar{x} = 0.3$, dotted line: $\bar{x} = 0.4$, dashed line: $\bar{x} = 0.5$

reaches larger values at such a t_z that D_{12} is immeasurable, which means that T_1, T_2 are virtually equal (measured in experiment) and $R_{21} = 1$ consequently, which has no use in the measurement.

At $H \leq 0.1$ and $a_x/a_z = 5$, the optimal values are $\bar{\Delta}_b = 0.2$ and $\bar{x} = 0.8$. Then, $S_{21\,\max} \approx 0.6$. (We have excluded the larger values of $\bar{x}$ from the investigation because of the possible influence of heat losses from the lateral surfaces of the sample.) If we consider $S_{21\,\max} \approx 0.3$ sufficient, then $\bar{\Delta}_b = 0.1$ and $\bar{x} = 0.2$ are the optimal values in general. In any case, functions R_{21} and R_{23} reach values around 0.5 at the optimal $\bar{\Delta}_b$ and $\bar{x}$. Thus, these parts of R_{21} and R_{23} are crucial for the determination of the diffusivities.

As $a_z \approx 10^{-7}\mathrm{m}^2 \cdot \mathrm{s}^{-1}$, $e \approx 10^{-3}\mathrm{m}$, and $t = \frac{e^2}{a_z} t_z$ (see Eq. 5), then $t \approx 10 t_z$. If $a_x/a_z = 0.2$ and $H = 1$, then $t_{z\,S21\,\max} = 1.31$ and $t_{z\,S23\,\max} = 0.17$. If $a_x/a_z = 1$ and $H = 1$, then $t_{z\,S21\,\max} = 0.26$ and $t_{z\,S23\,\max} = 0.17$. If $a_x/a_z = 5$ and $H = 1$, then $t_{z\,S21\,\max} = 0.05$ and $t_{z\,S23\,\max} = 0.17$. If $a_x/a_z = 0.2$ and $H = 0.1$, then $t_{z\,S21\,\max} = 1.31$ and $t_{z\,S23\,\max} = 0.19$. These are all reasonable times.

To compute the diffusivity a_x at the optimal $\bar{\Delta}_b$ and $\bar{x}$, we use the method of least squares for Eq. 8. Let N be the number of measured points $[t_i, T_1\,(t_i)]$, $[t_i, T_2\,(t_i)]$, and $[t_i, T_3\,(t_i)]$. We are looking for the value of a_x at which the sum,

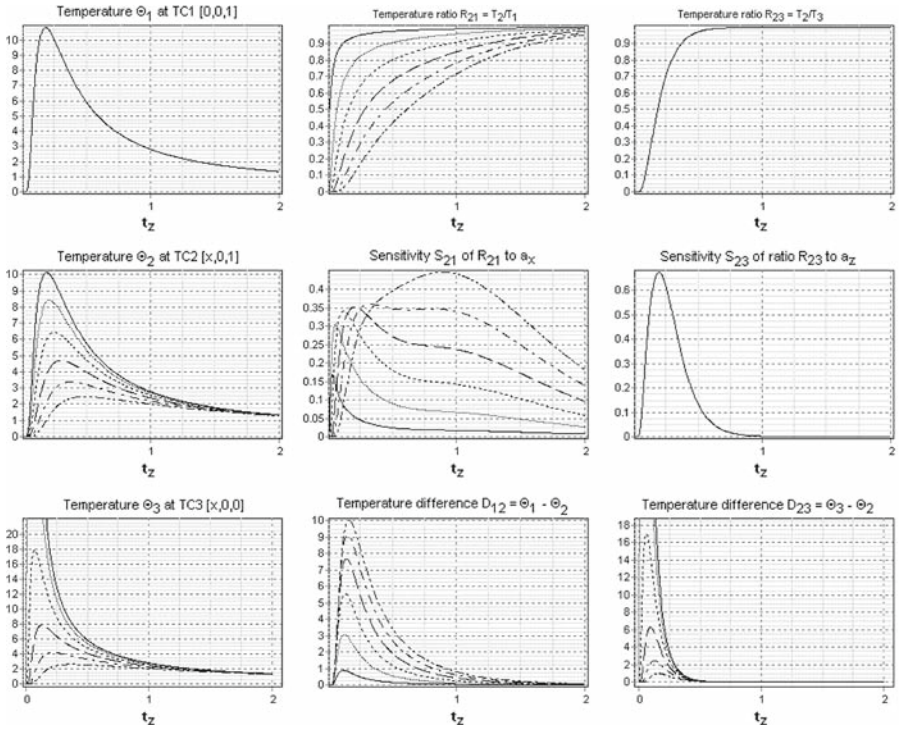

Fig. 12 Functions Θ_1, Θ_2, Θ_3, R_{21}, S_{21}, D_{12}, R_{23}, S_{23}, D_{23} at $e/b = 0.2$, $H = 0.1$, $a_x/a_z = 5$, $a_y/a_z = 1$, $\bar{\Delta}_b = 0.1$; normal line: $\bar{x} = 0.1$, small-dotted line: $\bar{x} = 0.2$, dotted line: $\bar{x} = 0.3$, dashed line: $\bar{x} = 0.4$, dashed-dotted line: $\bar{x} = 0.5$, dashed-dotted-dotted line: $\bar{x} = 0.6$

$$\sum_{i=1}^{N}\left[\frac{1+2\sum_{k=1}^{\infty}\cos\left(k\pi\bar{x}\right)\frac{\sin\left(k\pi\bar{\Delta}_b\right)}{k\pi\bar{\Delta}_b}\exp\left(-\pi^2k^2\frac{a_xt_i}{b^2}\right)}{1+2\sum_{k=1}^{\infty}\frac{\sin\left(k\pi\bar{\Delta}_b\right)}{k\pi\bar{\Delta}_b}\exp\left(-\pi^2k^2\frac{a_xt_i}{b^2}\right)}-\frac{T_2\left(t_i\right)}{T_1\left(t_i\right)}\right]^2 \tag{12}$$

is a minimum.

To compute a_z and H, we use the method of least squares on Eq. 9, i.e., we are looking for the values of a_z and H at which the sum,

$$\sum_{i=1}^{N}\left[\frac{\sum_{n=1}^{\infty}a_n\left[\cos\left(u_n\right)+\frac{H}{u_n}\sin\left(u_n\right)\right]\exp\left(-u_n^2\frac{a_zt}{e^2}\right)}{\sum_{n=1}^{\infty}a_n\exp\left(-u_n^2\frac{a_zt}{e^2}\right)}-\frac{T_2\left(t_i\right)}{T_3\left(t_i\right)}\right]^2 \tag{13}$$

is a minimum. The minimum problems are readily solvable by a PC program.

Here we note that the initial temperature of the sample has a non-zero value in a real experiment despite the fact that the theory assumes that it is zero. This so-called baseline temperature has to be taken into account in the data reduction. Our practical experiences show that it is better to estimate the baseline temperature and recalculate

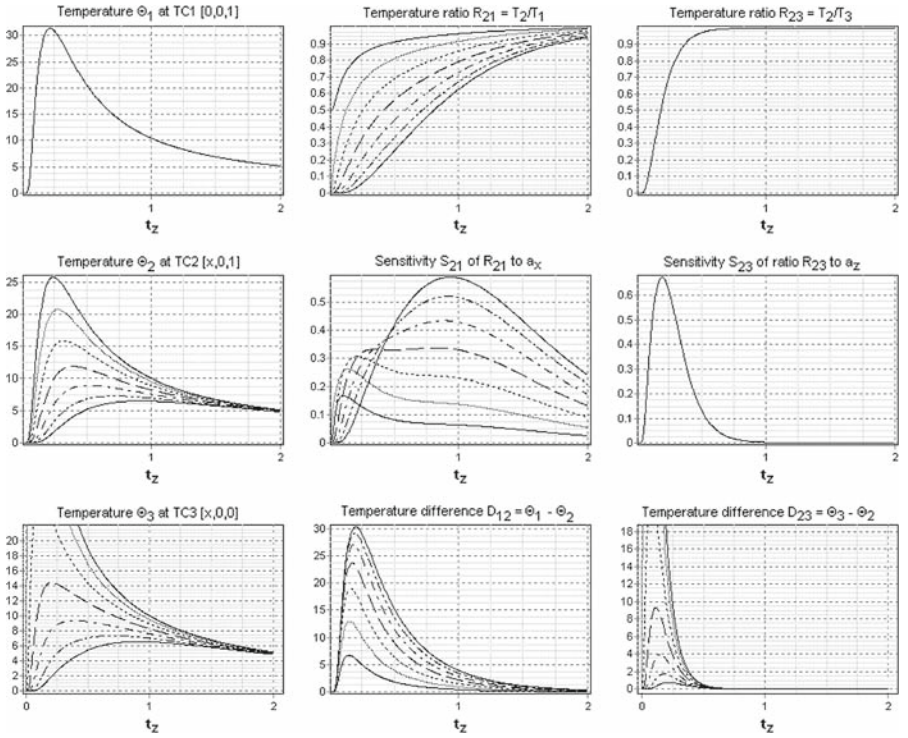

Fig. 13 Functions Θ_1, Θ_2, Θ_3, R_{21}, S_{21}, D_{12}, R_{23}, S_{23}, D_{23} at $e/b = 0.2$, $H = 0.1$, $a_x/a_z = 5$, $a_y/a_z = 1$, $\bar{\Delta}_b = 0.2$; normal line: $\bar{x} = 0.2$, small-dotted line: $\bar{x} = 0.3$, dotted line: $\bar{x} = 0.4$, dashed line: $\bar{x} = 0.5$, dashed-dotted line: $\bar{x} = 0.6$, dashed-dotted-dotted line: $\bar{x} = 0.7$, normal line: $\bar{x} = 0.8$

the experimental temperature rise data prior to calculation than to obtain the baseline temperature by a least squares fitting.

4 Conclusions

This article describes a method for simultaneous measurements of the thermal diffusivities a_x, a_y, a_z of an orthotropic material. The method assumes a parallelepiped-shaped sample of square faces, thickness/width ratio = 0.2, heated on the front face on a coaxial square. The length of the side of the square is 10 % of the length of the side of the face. The temperature is measured at five points: in the center of the rear face, on the principal axes of the front face outside the heated area, and right opposite on the principal axes of the rear face (one rear central thermocouple and two front–rear pairs of thermocouples). The distance of the front sensor from the edge of the heated area is 20 % of the length of the side of the sample face.

Diffusivities a_x and a_y are computed using the method of least squares for the differences between the theoretical and experimental values of the ratio of the temperature on the corresponding principal axis and in the center—both on the rear face.

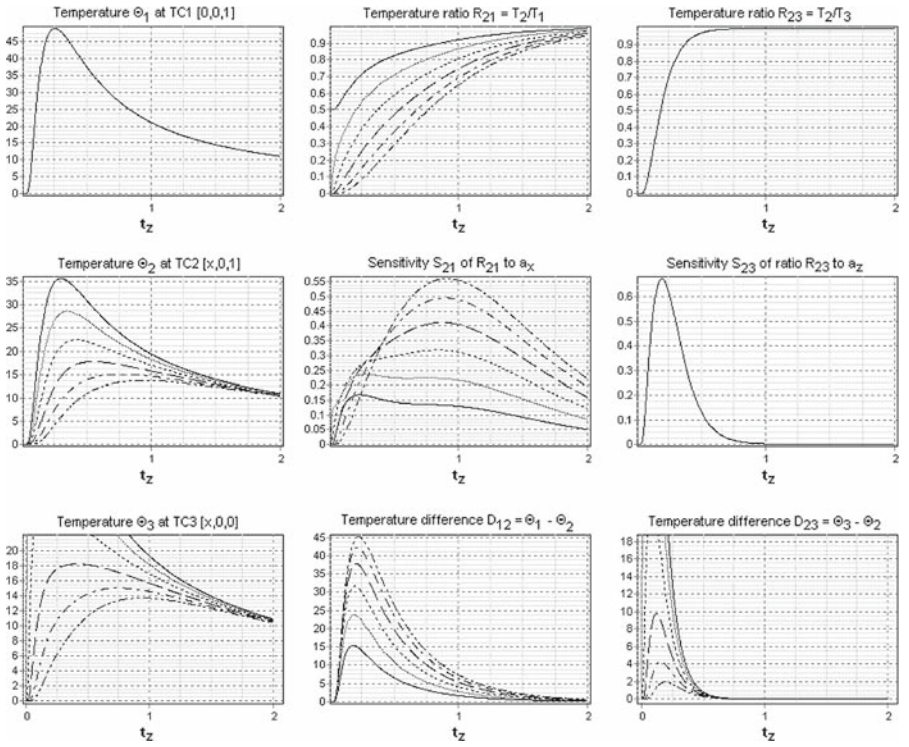

Fig. 14 Functions Θ_1, Θ_2, Θ_3, R_{21}, S_{21}, D_{12}, R_{23}, S_{23}, D_{23} at $e/b = 0.2$, $H = 0.1$, $a_x/a_z = 5$, $a_y/a_z = 1$, $\bar{\Delta}_b = 0.3$; normal line: $\bar{x} = 0.3$, small-dotted line: $\bar{x} = 0.4$, dotted line: $\bar{x} = 0.5$, dashed line: $\bar{x} = 0.6$, dashed-dotted line: $\bar{x} = 0.7$, dashed-dotted-dotted line: $\bar{x} = 0.8$

The thermal diffusivity a_z and the Biot number H can be obtained using the method of least squares over the theoretical and experimental values of front/rear temperature ratio on each principal axis of the faces. We get two values for either a_z or H, and we take the average of them for the exact value.

References

1. W.J. Parker, R.J. Jenkins, C.P. Butler, G.L. Abbott, J. Appl. Phys. **32**, 1679 (1961)
2. D.L. Balageas, High Temp. High Press. **21**, 85 (1989)
3. R.E. Taylor, K.D. Maglić, in *Compendium of Thermophysical Property Measurement Methods*, vol. 1, ed. by K.D. Maglić, A. Cezairliyan, V.E. Peletsky (Plenum, London, 1984), p. 305
4. L. Vozár, W. Hohenauer, High Temp. High Press. **35/36**, 253 (2003/2004)
5. F.I. Chu, R.E. Taylor, A.B. Donaldson, J. Appl. Phys. **51**, 336 (1980)
6. M. Lachi, A. Degiovanni, J. Phys. III France **1**, 2027 (1991)
7. A. Degiovanni, J.C. Batsale, D. Maillet, Rev. Gén. Therm. **35**, 141 (1996)
8. L. Vozár, T. Šrámková, High Temp. High Press. **29**, 183 (1997)
9. F. Mzali, L. Sassi, A. Jemni, S. Ben Nasrallah, D. Petit, High Temp. High Press. **35/36**, 281 (2003/2004)
10. F. Mzali, L. Sassi, A. Jemni, S. Ben Nasrallah, D. Petit, Inv. Probl. Sci. Eng. **12**, 193 (2004)
11. S. Graham, D.L. McDowell, R.B. Dinwiddie, Int. J. Thermophys. **20**, 691 (1999)
12. L. Vozár, J. Greguš, Š. Valovič, W. Hohenauer, in *Thermal Conductivity 27 and Thermal Expansion 15*, ed. by H. Wang, W. Porter (DEStech Publications, Inc., Lancaster, Pensylvania, 2004), p. 393